Supplementary Materials

S1. Charge density

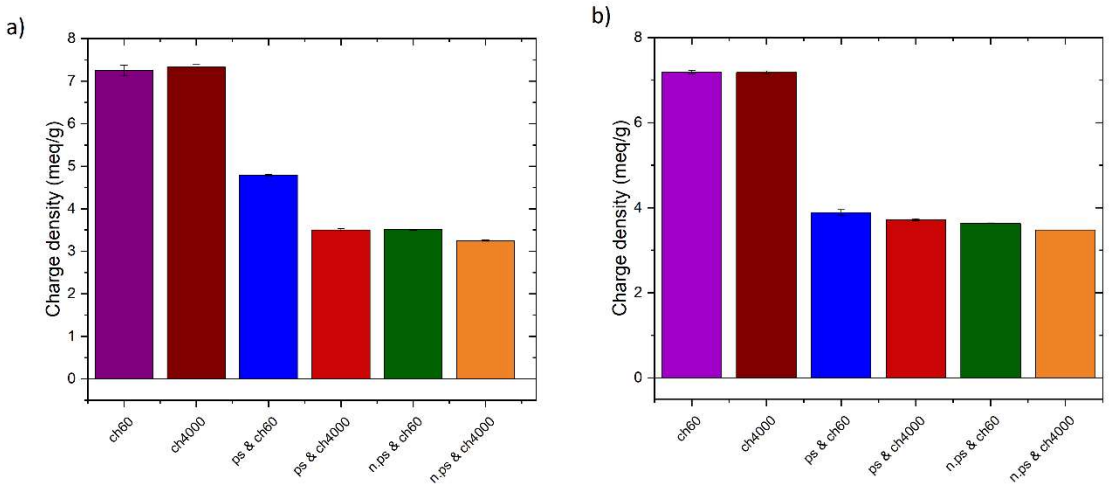

Figure S1. Charge densities of the different studied particles in dependence of pH of ch60 (purple), ch4000 (brown), ps & ch60 (dark blue), ps & ch4000 (red), n.ps & ch60 (green), and n.ps & ch4000 (orange) at (a) pH 1, and (b) pH 3.

S2. ATR-FTIR

Table S1. ATR-FTIR vibrations mode for chitosan-starch samples.

Wavenumber (cm^{-1})	Vibration mode
3350 - 3291	O-H, NH stretching, and intermolecular hydrogen bonding
2921	CH_2νas
2864	CH_2νs
1648	C-O stretching
1585	hydrogen bonding between OH and NH_3^+
1457-1417	CH_2 bending
1379	NH_2 bending (II), and C-O-O
1153-1060	C-O stretching
655	NH and OH bending

S3. BET-Measurments

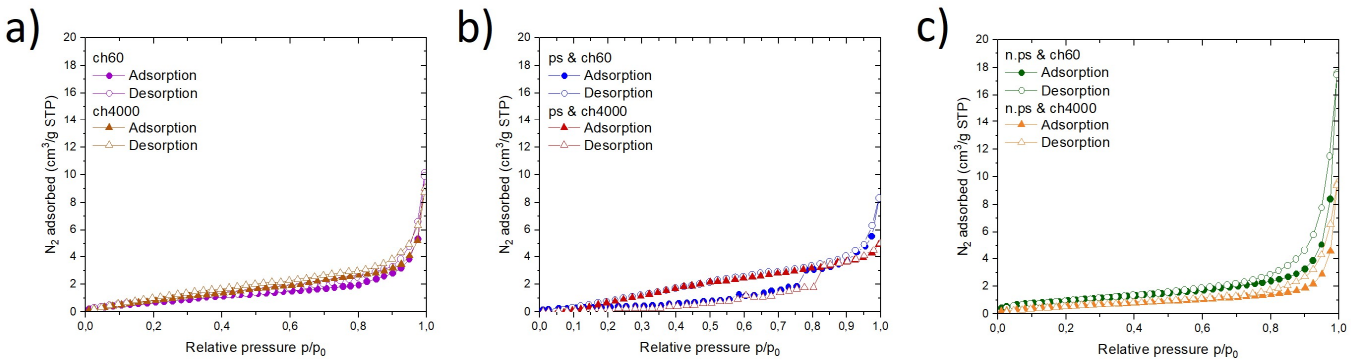

Figure S2. Nitrogen sorption isotherms at 77 K of (a) ch60 (purple), ch4000 (brown), (b) ps & ch60 (dark blue), ps & ch4000 (red), (c) n.ps & ch60 (green), and n.ps & ch4000 (orange).

Table S2. Surface area of the used samples using BET.

Sample	Surface area (m^2/g)
ch60	3
ch4000	4
ps & ch60	1
ps & ch4000	1
n.ps & ch60	3
n.ps & ch4000	4

S4. TGA of the samples

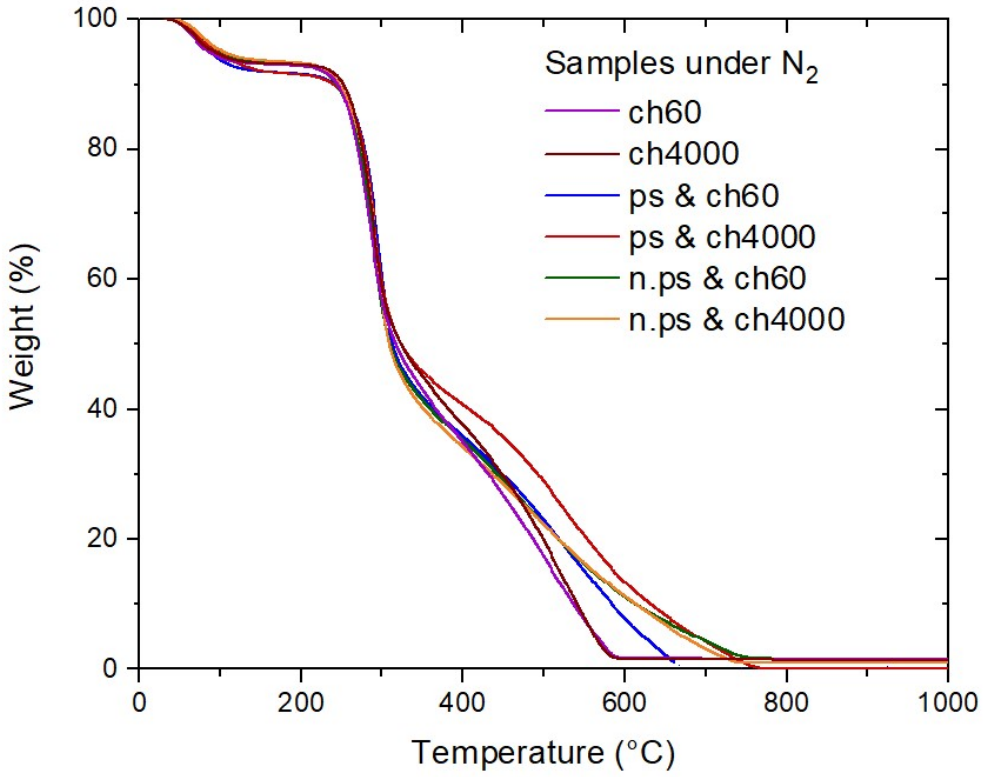

Figure S3. Thermogravimetric analysis under N_2 of ch60 (purple), ch4000 (brown), ps & ch60 (dark blue), ps & ch4000 (red), n.ps & ch60 (green), and n.ps & ch4000 (orange).

S5. Particle size distribution of n.ps in suspension

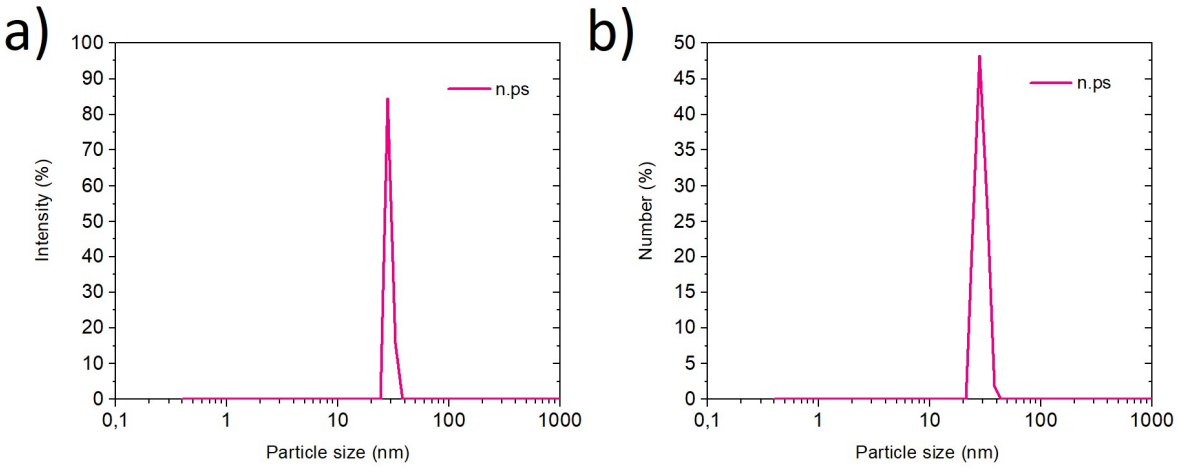

Figure S4. Particle size measurement of n.ps (a) intensity distribution and (b) number distribution.

S6. SEM-EDX analyses of samples before adsorption

S6.1. SEM-EDX elemental mappings from ps & ch60

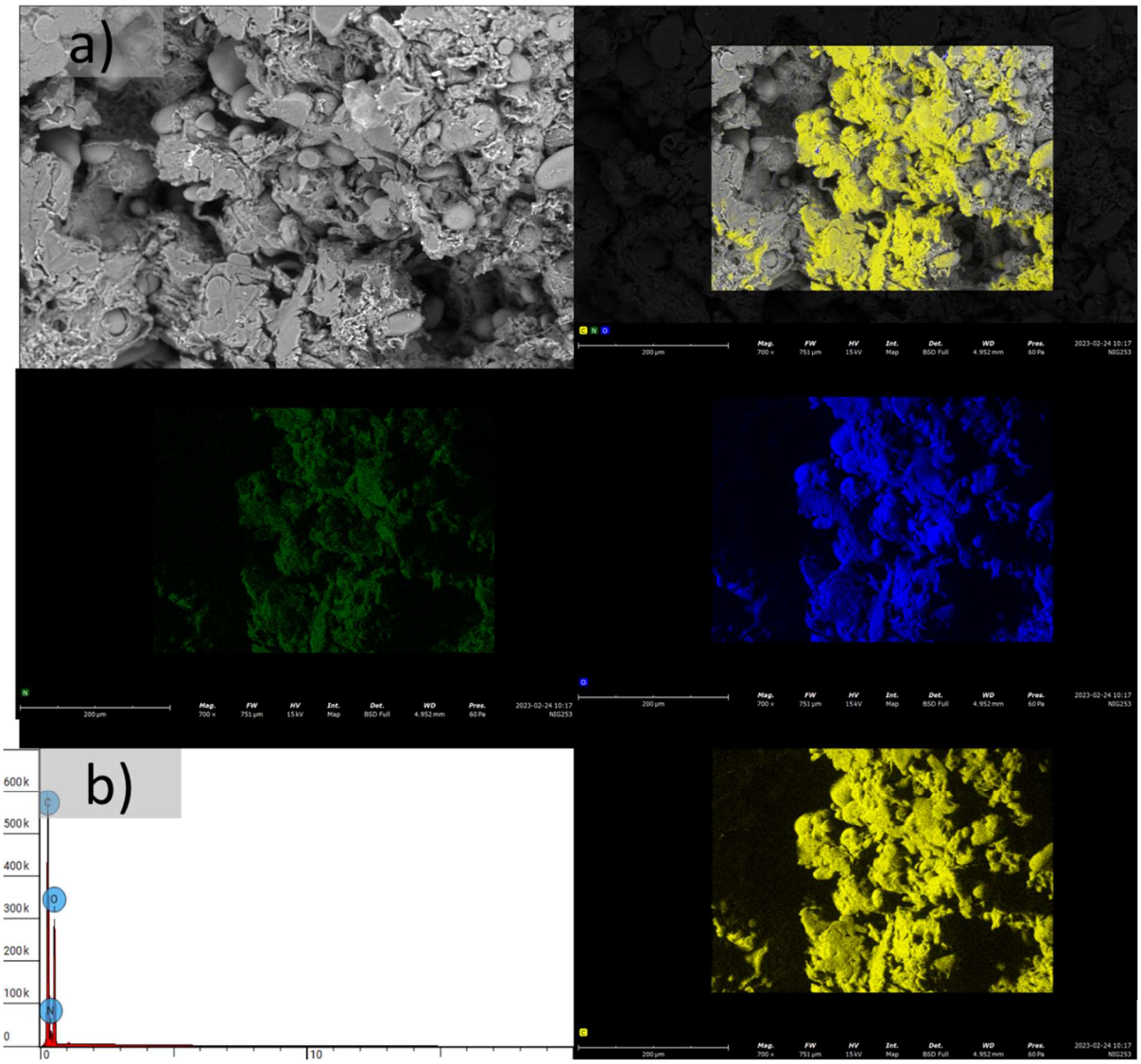

Figure S5. (a) SEM images and SEM-EDX elemental mappings from ps & ch60,(b) sum spectrum.

Table S3. Percent atomic and weight concentrations of iron and sulfur onto the surface area of ps & ch60.

Element Number	Element Symbol	Element Name	Atomic Conc. (%)	Weight Conc. (%)
6	C	Carbon	45.046	39.117
7	N	Nitrogen	18.714	18.957
8	O	Oxygen	36.240	41.926

S6.2. SEM images and SEM-EDX elemental mappings from ps & ch4000

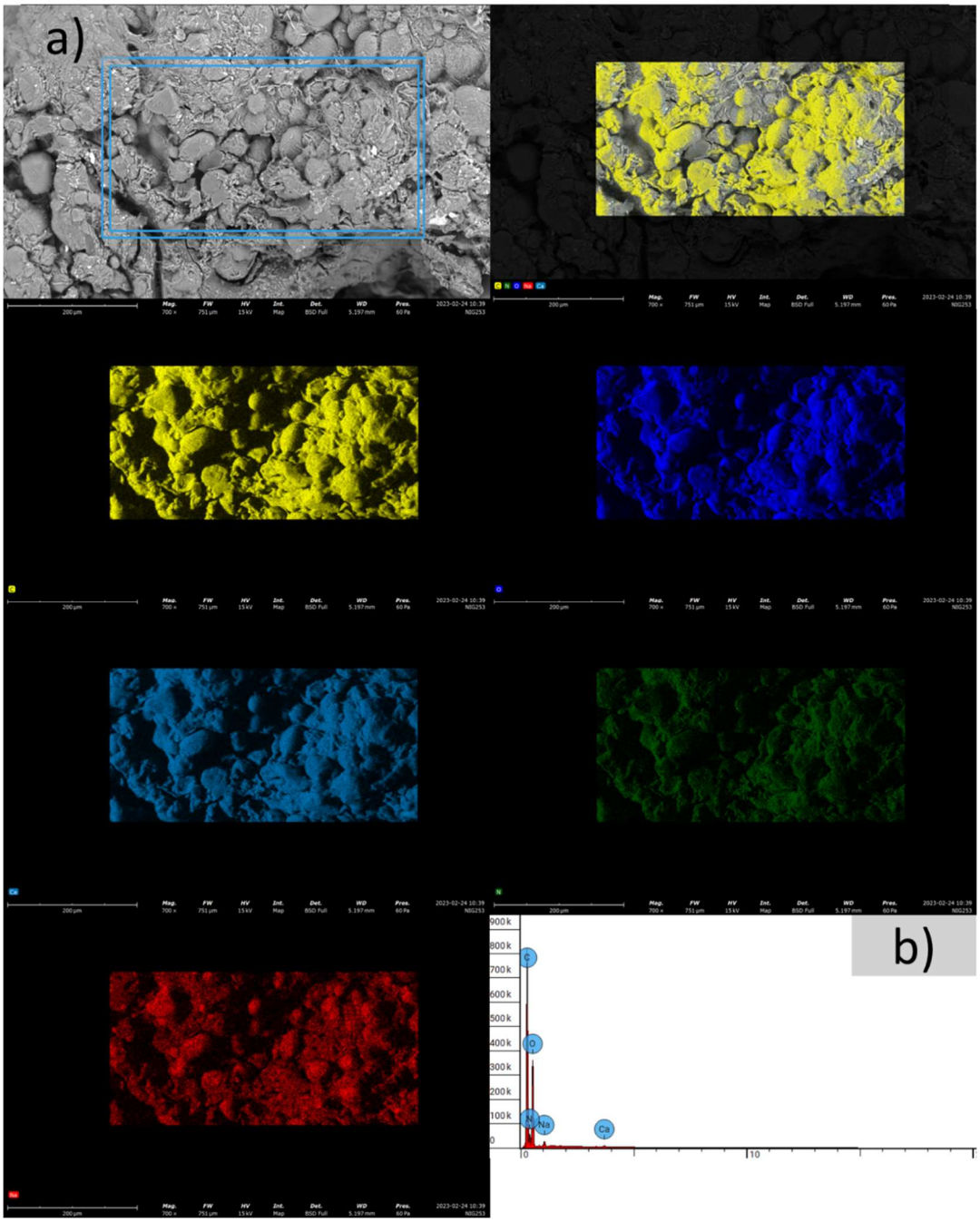

Figure S6. (a) SEM images and SEM-EDX elemental mappings from ps & ch4000,(b) sum spectrum.

Table S4. Percent atomic and weight concentrations of iron and sulfur onto the surface area of ps & ch4000.

Element Number	Element Symbol	Element Name	Atomic Conc. (%)	Weight Conc. (%)
6	C	Carbon	42.033	36.000
7	N	Nitrogen	18.917	18.900
8	O	Oxygen	38.387	43.800
11	Na	Sodium	0.488	0.800

S6.3. SEM images and SEM-EDX elemental mappings from n.ps & ch60

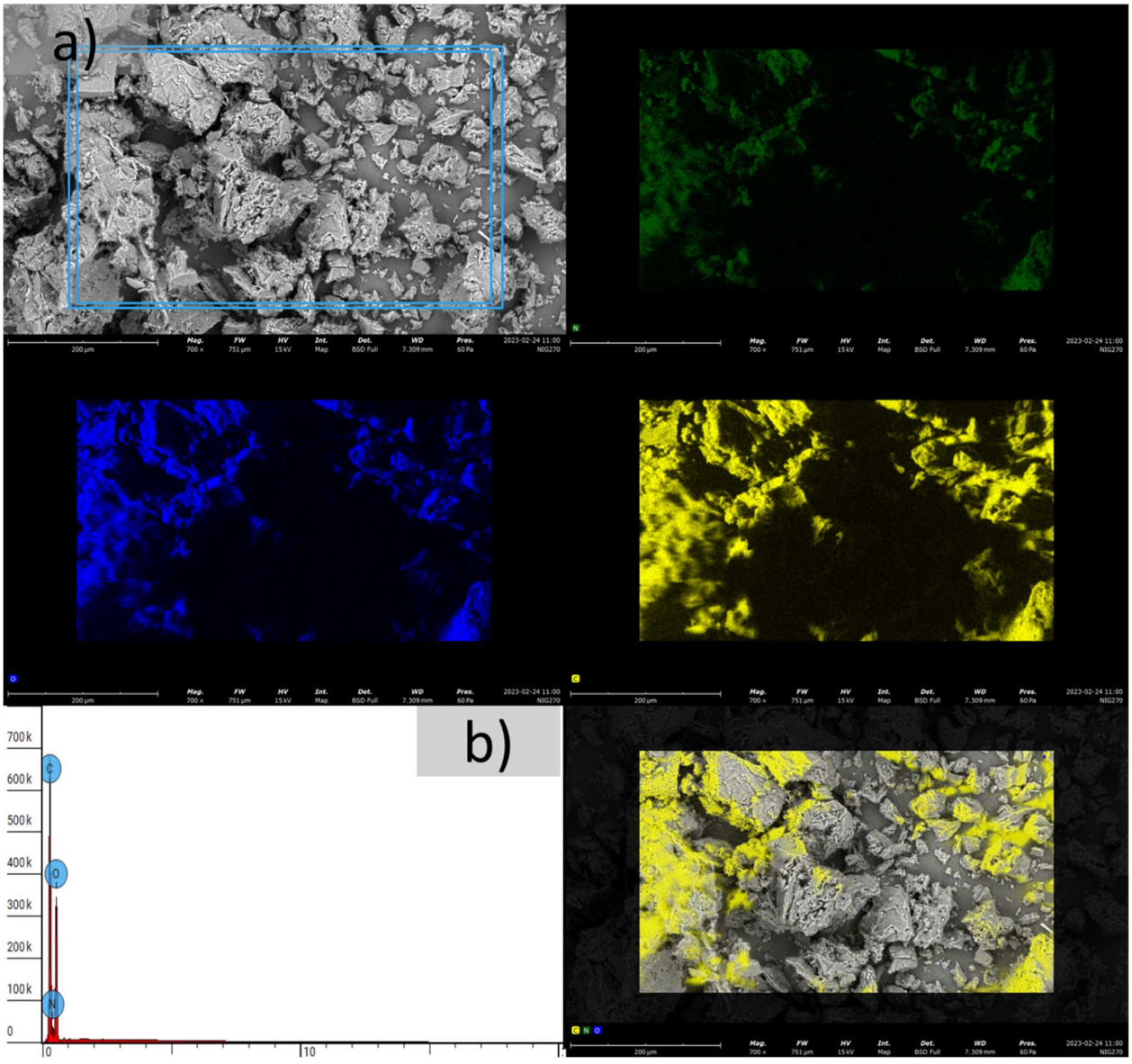

Figure S7. (a) SEM images and SEM-EDX elemental mappings from n. ps & ch60,(b) sum spectrum.

Table S5. Percent atomic and weight concentrations of iron and sulfur onto the surface area of n.ps & ch60.

Element Number	Element Symbol	Element Name	Atomic Conc. (%)	Weight Conc. (%)
6	C	Carbon	46.011	39.980
7	N	Nitrogen	17.201	17.435
8	O	Oxygen	36.788	42.585

S6.4. SEM images and SEM-EDX elemental mappings from n.ps & ch4000

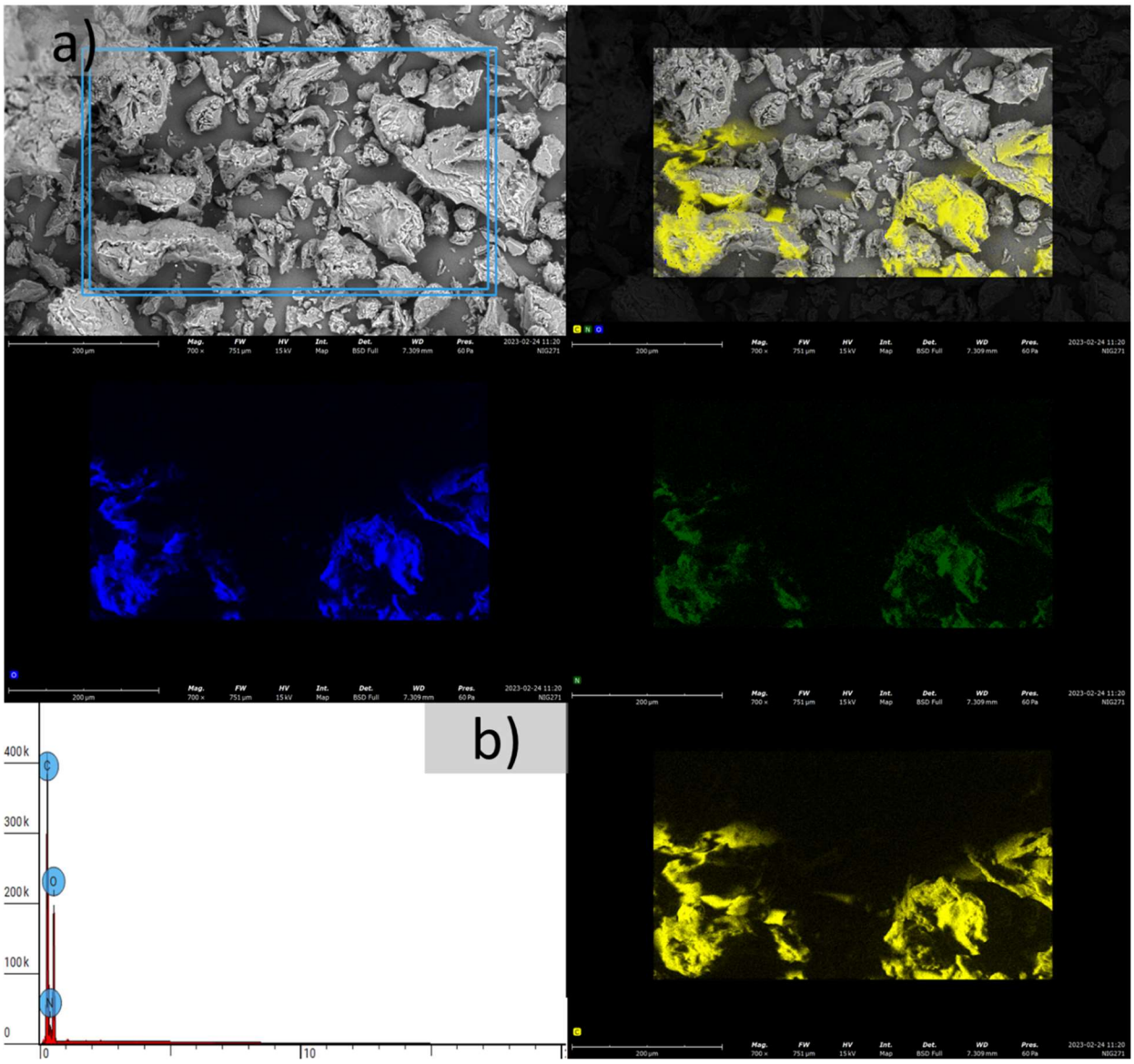

Figure S8. (a) SEM images and SEM-EDX elemental mappings from n. ps & ch4000,(b) sum spectrum.

Table S6. Percent atomic and weight concentrations of iron and sulfur onto the surface area of n.ps & ch4000.

Element Number	Element Symbol	Element Name	Atomic Conc. (%)	Weight Conc. (%)
6	C	Carbon	45.262	39.357
7	N	Nitrogen	19.202	19.478
8	O	Oxygen	35.535	41.165

S7. SEM-EDX analyses of samples after adsorption

S7.1. SEM-EDX elemental mappings from ps & ch60

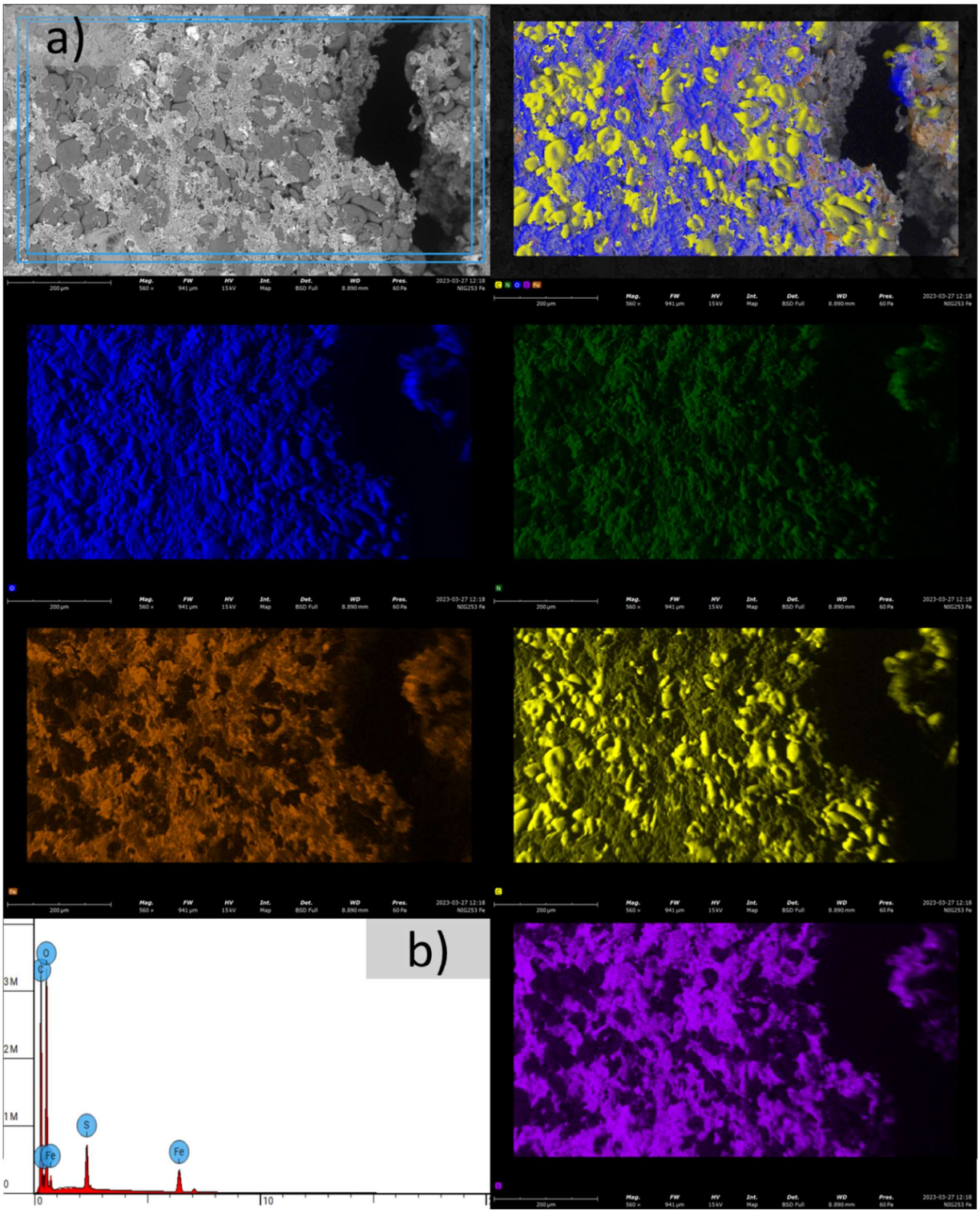

Figure S9. (a) SEM images and SEM-EDX elemental mappings from ps & ch60,(b) sum spectrum at a concentration of $Fe^{2+/3+}$ 1000 mg/L.

Table S7. Percent atomic and weight concentrations of iron and sulfur onto the surface area of ps & ch60.

Element Number	Element Symbol	Element Name	Atomic Conc. (%)	Weight Conc. (%)
6	C	Carbon	48.090	37.400
8	O	Oxygen	47.776	49.500
16	S	Sulfur	1.204	2.500
26	Fe	Iron	2.931	10.600

S7.2. SEM-EDX elemental mappings from ps & ch4000

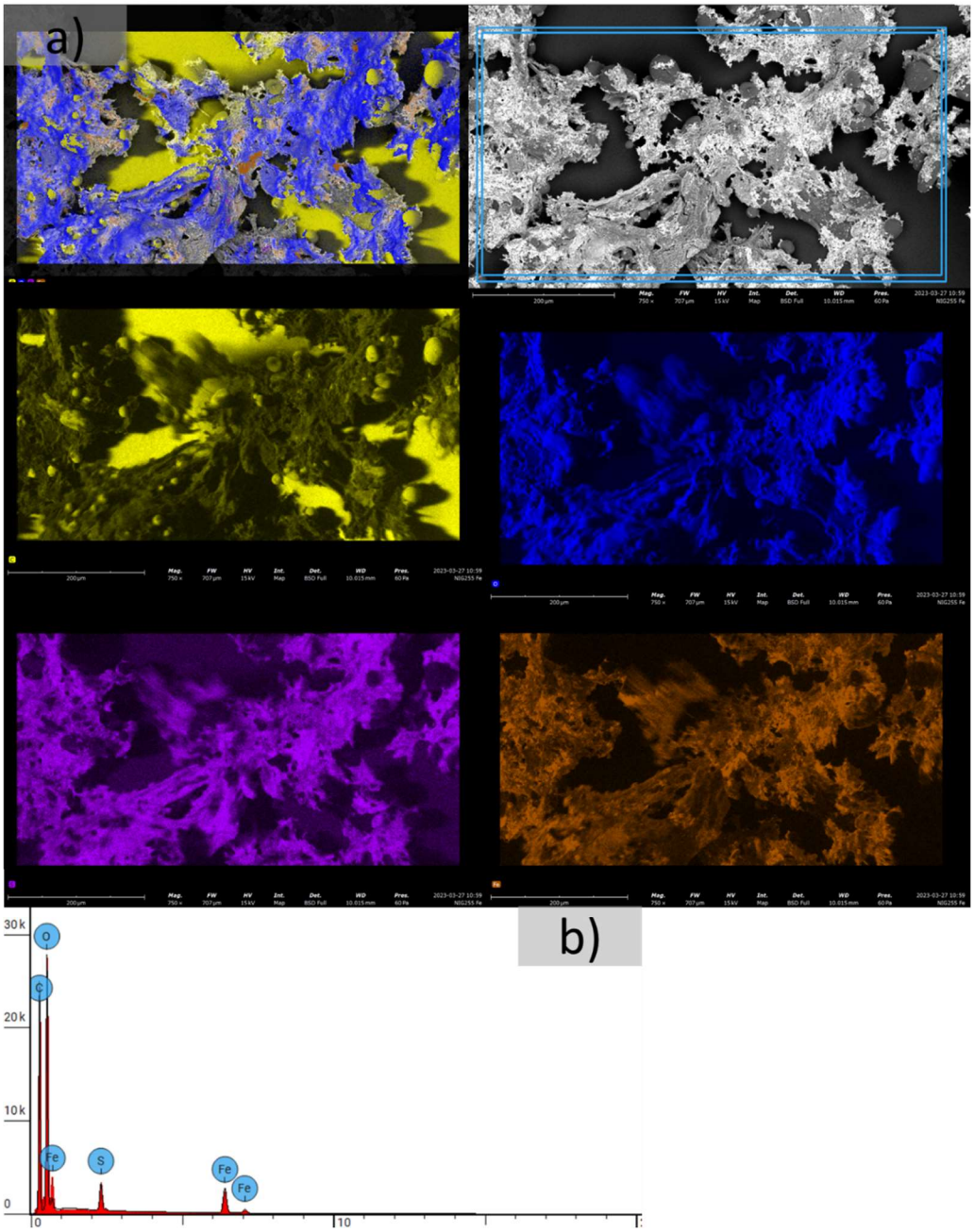

Figure S10. SEM images and SEM-EDX elemental mappings from ps & ch4000,(b) sum spectrum at a concentration of $Fe^{2+/3+}$ 1000 mg/L.

Table S8. Percent atomic and weight concentrations of iron and sulfur onto the surface area of ps & ch4000.

Element Number	Element Symbol	Element Name	Atomic Conc. (%)	Weight Conc. (%)
6	C	Carbon	59.357	44.845
8	O	Oxygen	34.013	34.234
16	S	Sulfur	1.588	3.203
26	Fe	Iron	5.043	17.718

S7.3. SEM-EDX elemental mappings from n.ps & ch60

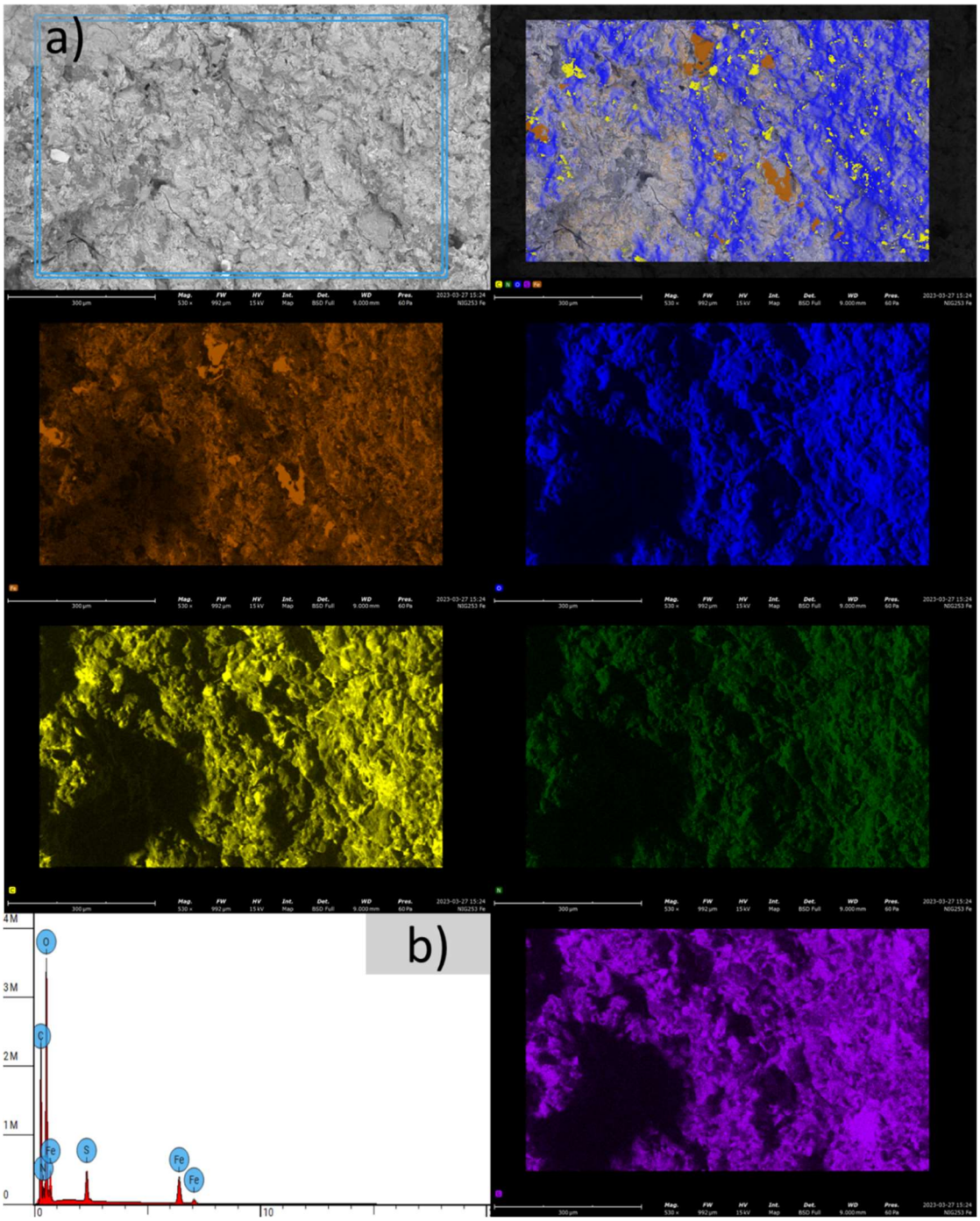

Figure S11. SEM images and SEM-EDX elemental mappings from n.ps & ch60,(b) sum spectrum at a concentration of $Fe^{2+/3+}$ 1000 mg/L.

Table S9. Percent atomic and weight concentrations of iron and sulfur onto the surface area of n.ps & ch60.

Element Number	Element Symbol	Element Name	Atomic Conc. (%)	Weight Conc. (%)
6	C	Carbon	42.056	32.533
7	N	Nitrogen	8.098	7.307
8	O	Oxygen	45.264	46.647
16	S	Sulfur	1.938	4.004
26	Fe	Iron	2.644	9.510

S7.4. SEM-EDX elemental mappings from n.ps & ch4000

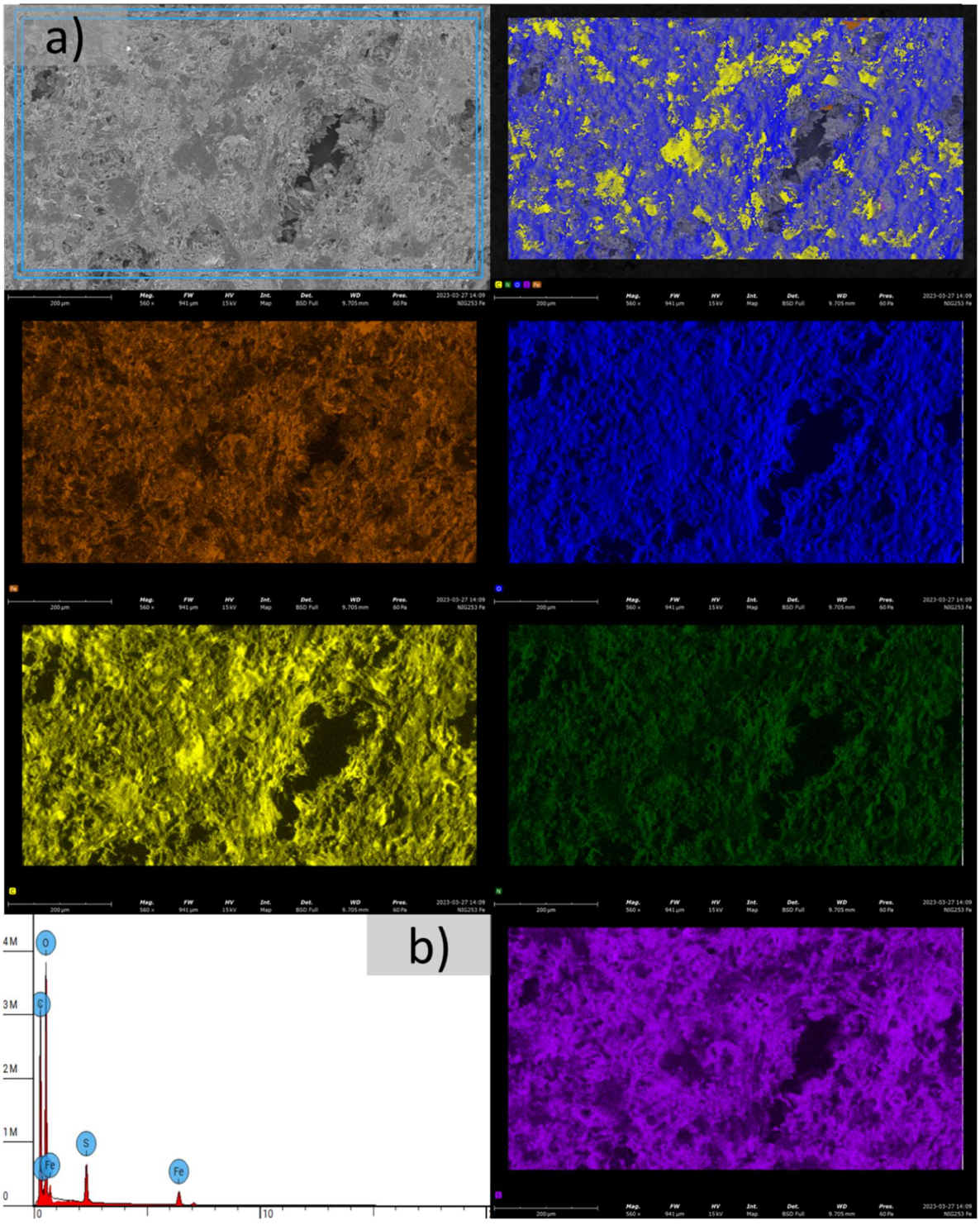

Figure S12. SEM images and SEM-EDX elemental mappings from n.ps & ch4000,(b) sum spectrum at a concentration of $Fe^{2+/3+}$ 1000 mg/L.

Table S10. Percent atomic and weight concentrations of iron and sulfur onto the surface area of n.ps & ch4000.

Element Number	Element Symbol	Element Name	Atomic Conc (%).	Weight Conc. (%)
6	C	Carbon	37.156	27.300
7	N	Nitrogen	11.667	10.000
8	O	Oxygen	45.155	44.200
16	S	Sulfur	1.427	2.800
26	Fe	Iron	4.595	15.700

S8. Change of color of samples

Figure S13. Change of color of samples at a concentration of iron 1000 mg/L and sulfate 1720 mg/L from $FeSO_4$ in dependence of time from 10 min to 24 h onto (a) ps. & ch60, (b) ps & ch4000, (c) n.ps & ch60, and (d) n.ps & ch4000 at room temperature and pH_0 4.26.

S9. Adsorption isotherms of $FeSO_4$ onto ch60 and ch4000

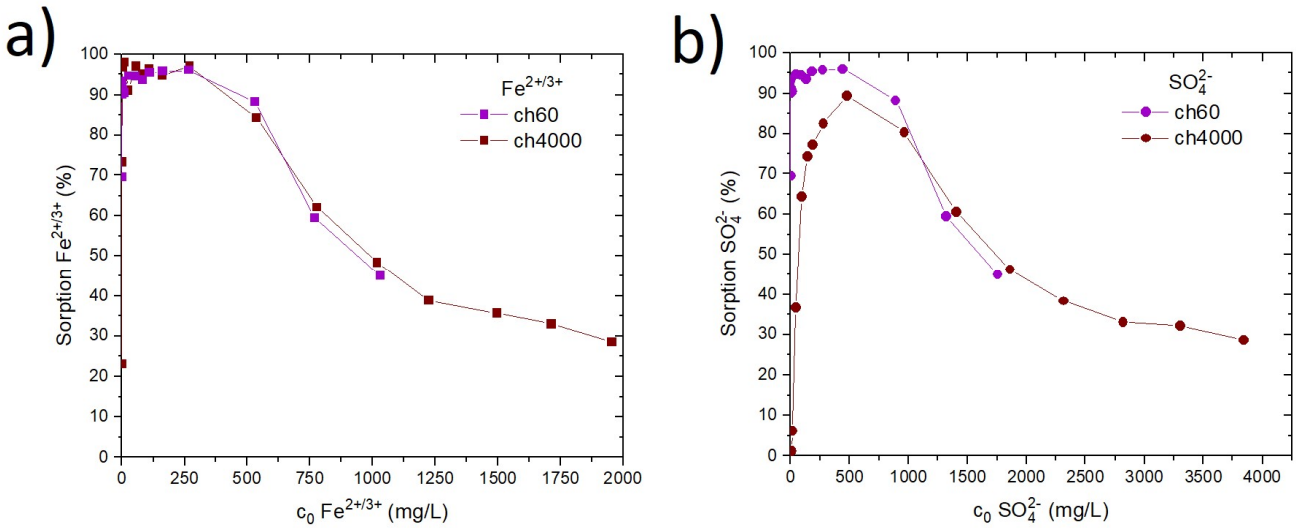

Figure S14. (a) Percentage adsorption of $Fe^{2+/3+}$ and (b)) percentage adsorption of SO_4^{2-} from $FeSO_4$ solution for ch60 (purple), and (b) ch4000 (brown).

S10. Adsorption capacity of ch60 and ch4000

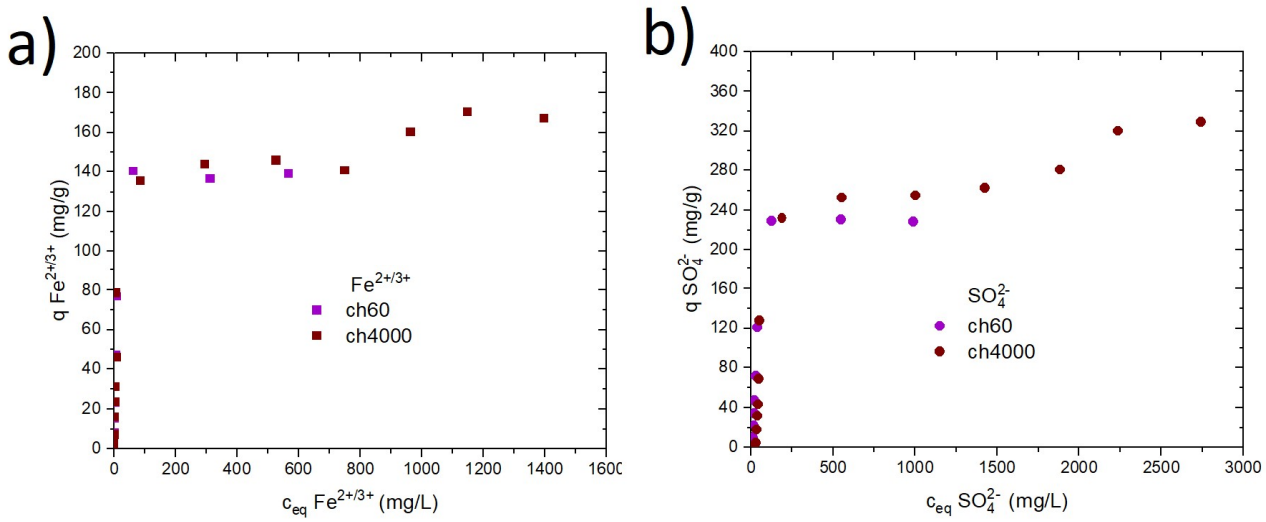

Figure S15. (a) Adsorption isotherm capacities for $Fe^{2+/3+}$ and (b)) Adsorption isotherms capacity for SO_4^{2-} from $FeSO_4$ solution for ch60 (purple), and (b) ch4000 (brown).

S11. pH values of ch60 and ch4000

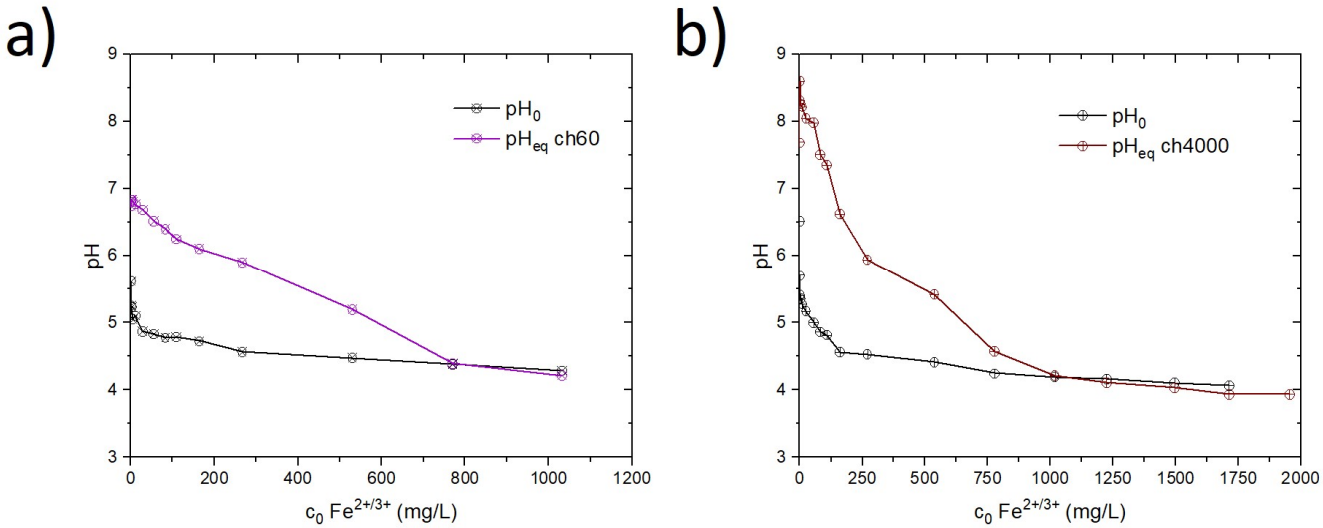

Figure S16. Corresponding pH_0 and pH_{eq} values from adsorption of $FeSO_4^{2-}$ onto (a) ch60 (purple), and (b) ch4000 (brown) with pH_0 (grey) corresponds to the pH value of the adsorptive solution before the experiment and pH_{eq} corresponds to the pH value after the adsorption process.

S12. Adsorption isotherms of $FeSO_4$ onto ps & ch60 (blue), ps & ch4000 (red), n.ps & ch60 (green), n.ps & ch4000 (orange).

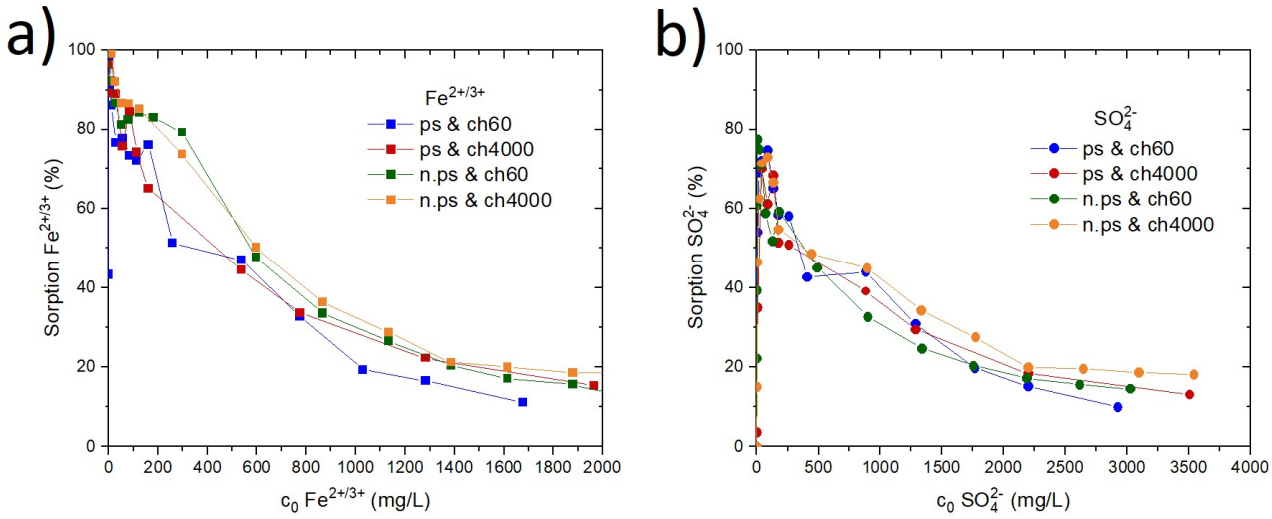

Figure S17. (a) percentage adsorption of $Fe^{2+/3+}$ and (b)) percentage adsorption of SO_4^{2-} from $FeSO_4$ solution with ps & ch60 (dark blue), ps & ch4000 (red), n.ps & ch60 (green), and n.ps & ch4000 (orange).

S13. pH Values of ps & ch60 (blue), ps & ch4000 (red), n.ps & ch60 (green), n.ps & ch4000 (orange).

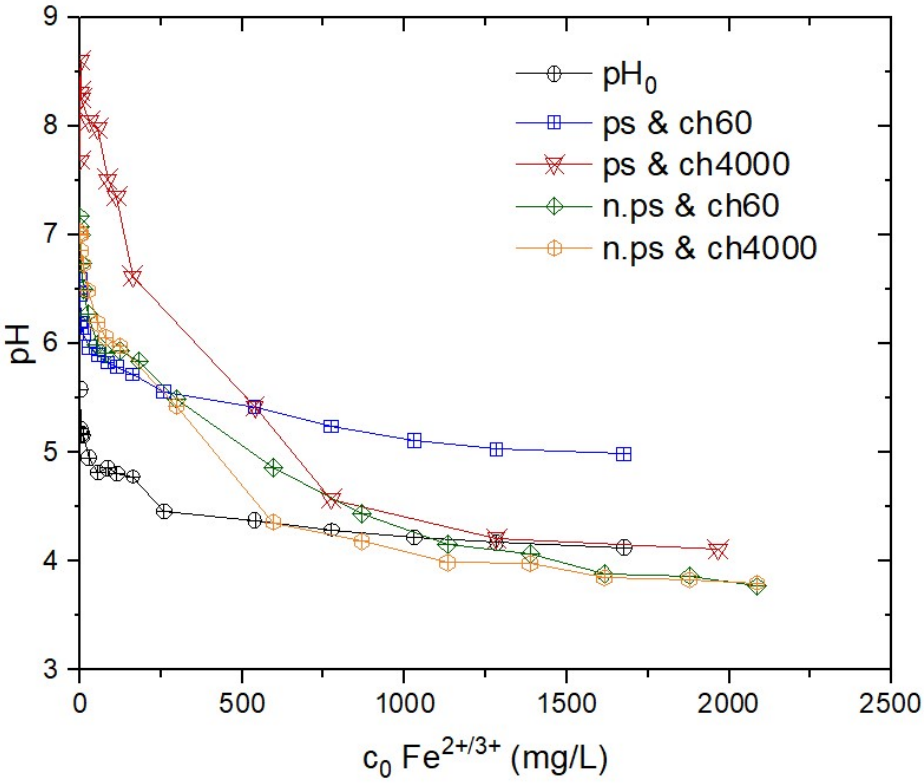

Figure S18. Corresponding pH_0 and pH_{eq} values from adsorption of $FeSO_4^{2-}$ onto ps & ch60 (dark blue), ps & ch4000 (red), n.ps & ch60 (green), and n.ps & ch4000 (orange). With pH_0 (grey) corresponds to the pH value of the adsorptive solution before the experiment and pH_{eq} corresponds to the pH value after the adsorption process.

S14. Adsorption isotherms fitted by Langmuir, Sips and Dubinin-Radushkevich.

S14.1. Langmuir Fitting Model

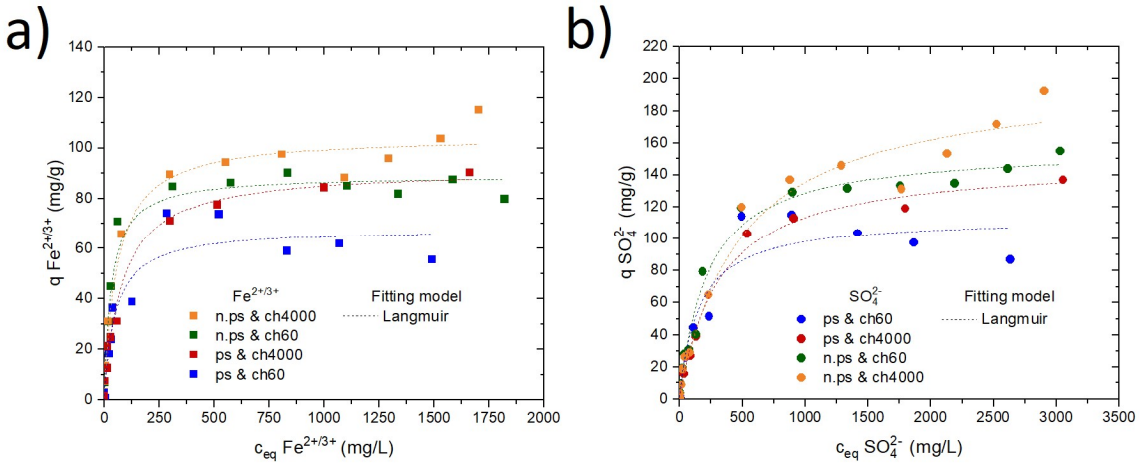

Figure S19. Adsorption isotherms capacity for (a) $Fe^{2+/3+}$, and (b) SO_4^{2-} from $FeSO_4$ solution and the respective Langmuir isotherm fitting model.

S14.2. Sips Fitting Model

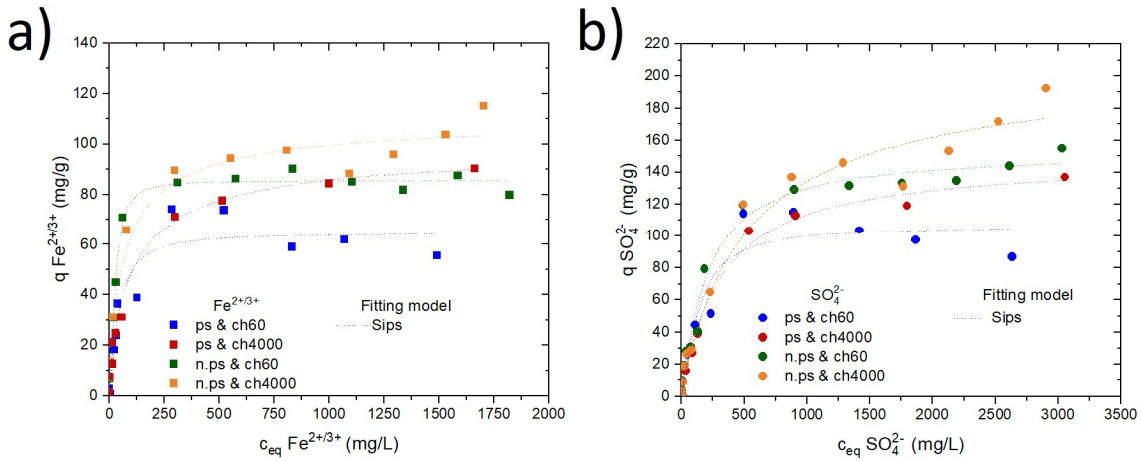

Figure S20. Adsorption isotherms capacity for (a) $Fe^{2+/3+}$, and (b) SO_4^{2-} from $FeSO_4$ solution and the respective Sips isotherm fitting model.

S14.3. Dubinin-Radushkevich Fitting Model

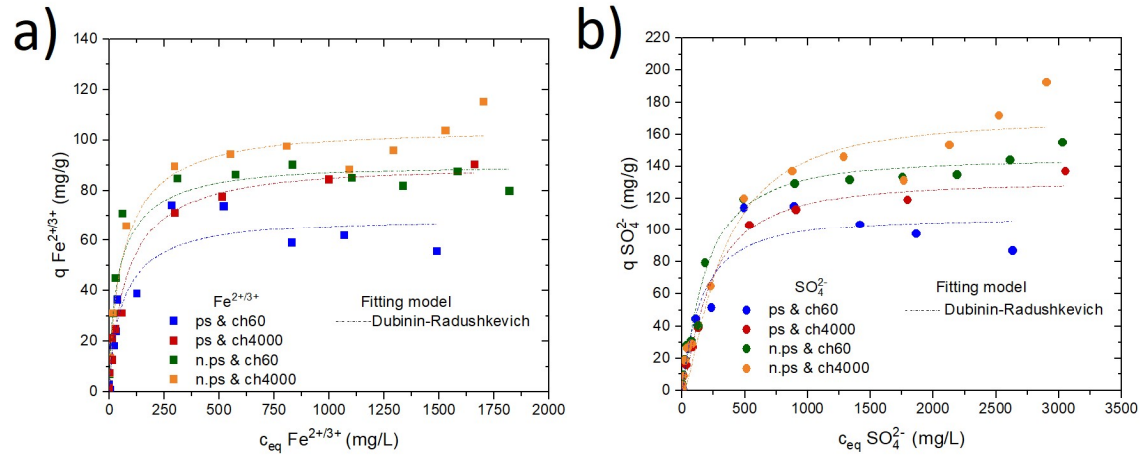

Figure S21. Adsorption isotherms capacity for (a) $Fe^{2+/3+}$, and (b) SO_4^{2-} from $FeSO_4$ solution and the respective Dubinin-Radushkevich isotherm fitting model.

Table S11. Fitting parameters for the adsorption of Fe^{2+} from $FeSO_4$ solution onto ps & ch60 (blue), ps & ch4000, n.ps & ch60, n.ps & ch4000 for Langmuir, Sips, and Dubinin-Radushkevich isotherm models.

Sample	Model	Q_m mg/g	K L/mg	$ß_{DR} \times 10^{-9}$ mol^2/J^2	n	$E_{ads,DR}$ KJ/mol	R^2 (COD)
ps & ch60	Langmuir	67.98 ± 4.10	0.019 ± 0.005	--	--		0.938
	Sips	64.60 ± 4.36	0.006 ± 0.009	--	1.35± 0.43	--	0.944
	Dubinin–Radushkevich	68.26 ± 3.87	--	13.2 ± 2.05	--	61.5± 4.79	0.933
ps & ch4000	Langmuir	91.65 ± 2.54	0.013 ± 0.001	--	--	--	0.990
	Sips	99.96 ± 5.80	0.024 ± 0.006	--	0.80 ± 0.08	--	0.993
	Dubinin–Radushkevich	88.83 ± 2.07	--	15.86 ± 9.5	--	56.14 ± 1.68	0.990
n.ps & ch60	Langmuir	89.05 ± 2.16	0.031± 0.004	--	--	--	0.983
	Sips	85.47 ± 1.09	0.0034 ± 0.001	--	1.72 ± 0.15	--	0.995
	Dubinin–Radushkevich	89.79 ± 2.71	--	10.51 ± 1.01	--	68.94.± 3.32.	0.972
n.ps & ch4000	Langmuir	104.98 ± 3.01	0.017 ± 0.002	--	--	--	0.981
	Sips	111.11 ± 7.08	0.032 ± 0.013	--	0.809 ± 0.13	--	0.983
	Dubinin–Radushkevich	103.53 ± 2.57	--	13.32 ± 1.15	--	61.43 ± 2.67	0.982

Table S12. Fitting parameters for the adsorption of SO_4^{2-} from $FeSO_4$ solution onto ps & ch60 (blue), ps & ch4000, n.ps & ch60, n.ps & ch4000 for Langmuir, Sips, and Dubinin–Radushkevich isotherm models.

Sample	Model	Q_m mg/g	K L/mg	$ß_{DR} \times 10^{-9}$ mol^2/J^2	n	$E_{ads,DR}$ KJ/mol	R^2 (COD)
ps & ch60	Langmuir	113.28 ±8.02	0.006 ± 0.001	--	--		0.936
	Sips	106.26 ±8.42	0.0012 ± 0.002	--	1.37 ± 0.4	--	0.943
	Dubinin–Radushkevich	107.32 ± 5.72	--	25.51 ± 4.09	--	44.26 ± 3.55	0.942
ps & ch4000	Langmuir	148.89 ± 5.12	0.003 ± 0.0003	--	--	--	0.990
	Sips	148.04 ± 9.07	0.0029 ± 0.001	--	1.01 ± 0.1	--	0.991
	Dubinin–Radushkevich	130.23 ± 4.25	--	38.2 ± 3.38	--	36.17 ± 1.60	0.982
n.ps & ch60	Langmuir	157.49 ± 4.47	0.004 ± 5.5	--	--	--	0.987
	Sips	153.1 ± 7.09	0.002 ± 0.001	--	1.09 ± 0.1	--	0.988
	Dubinin–Radushkevich	144.81 ± 3.32	--	31. 6± 2.58	--	39.74 ± 1.62	0.985
n.ps & ch4000	Langmuir	201.63 ± 12.41	0.002 ± 0.0004	--	--	--	0.971
	Sips	207.50 ± 31.04	0.002 ± 0.002	--	0.95 ± 0.2	--	0.970
	Dubinin–Radushkevich	169.54 ± 6.85	--	56.3 ± 8.17	--	29.79 ± 2.15	0.963

Table S13. Adsorption of iron ions onto biopolymers.

Materials	Adsorption capacity in mg/g	Salts	Experimental conditions			Ref.
			pH	a.d in g/L	t, T	
n.ps & ch4000	**115**	**$FeSO_4$**	5.6	3.33	24 h, 25˚C	This work
n.ps & ch60	90	$FeSO_4$	5.6	3.33	24 h, 25˚C	This work
ps & ch4000	80	$FeSO_4$	5.6	3.33	24 h, 25˚C	This work
ps & ch60	61	$FeSO_4$	5.6	3.33	24 h, 25˚C	This work
Ch85/400/A2	139	$FeSO_4 \cdot 7H_2O$ $FeSO_4$ (aq)	--	3.33	24 h, 25˚C	[34]
Native potato starch	0.65	$FeSO_4 \cdot 7H_2O$	5.4	3.33	2 h, 25 °C	[8]
Oxidized corn starch	3.58	$FeSO_4 \cdot 7H_2O$	5.4	3.33	2 h, 25 °C	[8]
Oxidized potato starch	4.34	$FeSO_4 \cdot 7H_2O$	5.4	3.33	2 h, 25 °C	[8]
Helles brewer's spent grain	10.2	$FeSO_4 \cdot 7H_2O$	5.5	3.33	24 h, 23 °C	[19]
Wheat beer brewer's spent grain	11.7	$FeSO_4 \cdot 7H_2O$	5.5	3.33	24 h, 23 °C	[19]

Table S14. Adsorption of sulfate ions onto biopolymers.

Materials	Adsorption capacity in mg/g	Salts	Experimental conditions			Ref
			pH	a.d in g/L	t, T	
n.ps & ch4000	**192**	**$FeSO_4$**	5.6	3.33	24 h, 25˚C	This work
n.ps & ch60	155	$FeSO_4$	5.6	3.33	24 h, 25˚C	This work
ps & ch4000	137	$FeSO_4$	5.6	3.33	24 h, 25˚C	This work
ps & ch60	97	$FeSO_4$	5.6	3.33	24 h, 25˚C	This work
Ch85/400/A2	220	$FeSO_4 \cdot 7H_2O$ $FeSO_4$ (aq)	--	3.33	24 h, 25˚C	[34]

References

8. Boughanmi, R.; Borchert, K.B.L.; Steinbach, C.; Mayer, M.; Schwarz, S.; Svirepa, A.; Schwarz, J.; Mertig, M.; Schwarz, D. Native and Oxidized Starch for Adsorption of Nickel, Iron, and Manganese Ions from Water. *Polysaccharides* **2022**, *3*, 556–573. https://doi.org/10.3390/polysaccharides3030033.

19. Carrasco, K.H.; Höfgen, E.G.; Brunner, D.; Borchert, K.B.L.; Reis, B.; Steinbach, C.; Mayer, M.; Schwarz, S.; Glas, K.; Schwarz, D. Removal of Iron, Manganese, Cadmium, and Nickel Ions Using Brewers' Spent Grain. Polysaccharides 2022, 3, 356–379, https://doi.org/10.3390/polysaccharides3020021.

34. Weißpflog, J.; Gündel, A.; Vehlow, D.; Steinbach, C.; Müller, M.; Boldt, R.; Schwarz, S.; Schwarz, D. Solubility and Selectivity Effects of the Anion on the Adsorption of Different Heavy Metal Ions onto Chitosan. *Molecules* **2020**, *25*, 2482. https://doi.org/10.3390/molecules25112482.